APPROXIMATE PROBABILISTIC OPTIMIZATION OF A WINGBOX MODEL USING EXACT-CAPACITY-APPROXIMATE-RESPONSE-DISTRIBUTION (ECARD)

By

RICHARD J. PIPPY

A THESIS PRESENTED TO THE GRADUATE SCHOOL
OF THE UNIVERSITY OF FLORIDA IN PARTIAL FULFILLMENT
OF THE REQUIREMENTS FOR THE DEGREE OF
MASTER OF SCIENCE

UNIVERSITY OF FLORIDA

2008

To my parents, Richard and Evelyn, and to my brother Chris

ACKNOWLEDGMENTS

I would like to express my sincere gratitude to my advisor and the chair of my thesis committee, Dr. Nam-Ho Kim, and to the co-chair, Dr. Rafael T. Haftka, for their guidance, enthusiasm and continual support throughout my study. I am also grateful to committee member Dr. Peter G. Ifju for his advice and patience in reviewing this thesis. Special thanks go to Mulu Haile for his help in deriving the wingbox load conditions. I would like to thank my colleagues in the Structural and Multidisciplinary Optimization Lab at the University of Florida, in particular, Sunil Kumar, Dr. Erdem Acar, Palani Ramu, Haoyu Wang and Saad M. Mukras for their help and encouragement.

TABLE OF CONTENTS

LIST OF TABLES

LIST OF FIGURES

Abstract of Thesis Presented to the Graduate School
of the University of Florida in Partial Fulfillment of the
Requirements for the Degree of Master of Science

APPROXIMATE PROBABILISTIC OPTIMIZATION OF A WINGBOX MODEL USING EXACT-CAPACITY-RESPONSE-DISTRIBUTION (ECARD)

By

Richard J. Pippy

May 2008

Chair: Nam-Ho Kim
Co-chair: Rafael T. Haftka
Major: Mechanical Engineering

There are two major obstacles that affect probabilistic (or reliability-based) structural optimization. First, uncertainties associated with errors in structural and aerodynamic modeling and quality of construction are not well characterized as statistical distributions and it has been shown that insufficient information may lead to large errors in probability calculations. Second, probabilistic optimization is computationally expensive due to multiple analyses, typically finite element analyses, for calculating probability as the structure is being redesigned. In order to overcome these obstacles, we propose an approximate probabilistic optimization method where the probabilistic calculation is confined to failure stress. This takes advantage of the fact that statistical characterization of failure stresses is required by Federal Aviation Administration regulations. The need for expensive stress distribution calculations are eliminated by condensing the stress distribution into a representative deterministic value, transforming a probabilistic optimization problem into a semi-deterministic optimization problem. By starting the approximate probabilistic optimization from the deterministic optimum design, a small number of iterations is expected and reliability analysis is required only once per iteration. This proposed method provides approximate sensitivity of failure probability with respect to the design

variables, which is essential in risk allocation. This method is demonstrated in two examples. The first example uses a ten-bar truss which demonstrates the risk allocation between the truss elements. The second example uses a wingbox model based on a Boeing 767-400 aircraft which demonstrates the risk allocation between two different failure modes of stress and displacement.

CHAPTER 1
INTRODUCTION

There are two major barriers in front of probabilistic (or reliability-based) structural optimization. First, uncertainties associated with material properties, operating conditions, mathematical models, and manufacturing variability are not well characterized as statistical distributions, and insufficient information may lead to large errors in probability calculations (e.g., Ben-Haim and Elishakoff [1], Neal, et al. [2]). Due to this fact, many engineers are reluctant to pursue probabilistic design. The second barrier to the application of probabilistic structural optimization is computational expense. Probabilistic structural optimization is expensive because repeated stress calculations (typically FEA) are required for updating probability calculation as the structure is being re-designed. Targeting these two main barriers, we propose an approximate probabilistic optimization method that dispenses with expensive probabilistic stress calculations. In the proposed method, the probabilistic calculation is confined only to failure stress, which is often well characterized.

Traditionally, reliability-based design optimization (RBDO) is performed based on a double-loop optimization scheme, where the outer loop is used for design optimization while the inner loop performs a sub-optimization for reliability analysis, using methods such as First-Order Reliability Method (FORM). Since this traditional approach is computationally expensive, even prohibitive for problems that require complex finite element analysis (FEA), alternative methods have been proposed by many researchers (e.g., Lee and Kwak [3], Kiureghian et al. [4], Tu et al. [5], Lee et al. [6], Qu and Haftka [7], Du and Chen [8] and Ba-abbad et al. [9]). These methods replace the probabilistic optimization with sequential deterministic optimization (often using inverse reliability measures) to reduce the computational expense. However, these approaches do not necessarily converge to the optimum design, and they do not easily lend themselves to

allocating risk between failure modes in a structure where many components can fail [10]. We note, however, that most of the computational expense is associated with repeated stress calculation.

So we propose an approximate probabilistic design approach that reduces the number of expensive stress calculations. That is, we approximate the probabilistic optimization that separates the uncertainties which can be evaluated inexpensively and those whose effects are expensive to evaluate. We boil down the stress distribution to a single characteristic stress by utilizing the inverse cumulative distribution of the failure stress, and we propose an inexpensive approximation of that characteristic stress. This proposed method will also improve upon a deterministic design by reallocating the safety margins between different components or failure modes. We call the proposed approximate probabilistic optimization approach Exact-Capacity-Approximate-Response-Distribution or ECARD. The purpose of this thesis is to further advance the version of ECARD which was originally developed by Dr. Erdem Acar and Dr. Rafael T. Haftka [11]. There is now an improved version of ECARD which was developed by Sunil Kumar, Dr. Rafael T. Haftka, and Dr. Nam-Ho Kim.

The remainder of the thesis is organized as follows. Chapter 2 discusses the theory behind the ECARD method. The application of the method to a ten-bar truss problem is presented in Chapter 3 and a wingbox design in Chapter 4. Finally, the concluding remarks are listed Chapter 5.

CHAPTER 2
EXACT-CAPACITY-RESPONSE-DISTRIBUTION (ECARD) THEORY

Introduction

In this chapter, the approximate probabilistic optimization method, named ECARD, will be discussed.

Characteristic Response

In probabilistic optimization, the system constraint is often given in terms of failure probability of a performance function. We consider a specific form of performance function, given as

$$g(\mathbf{x};\mathbf{u}) = c(\mathbf{x};\mathbf{u}) - r(\mathbf{x};\mathbf{u}) \tag{2-1}$$

where $c(\mathbf{x};\mathbf{u})$ and $r(\mathbf{x};\mathbf{u})$ are capacity and response, respectively. Both the capacity and response are random because they are functions of input random variables $\mathbf{x}$ and depend on deterministic design variables $\mathbf{u}$. The system is considered to be failed when the response exceeds the capacity; i.e., $g(\mathbf{x}; \mathbf{u}) < 0$. We assume that the probabilistic distribution of $c(\mathbf{x};\mathbf{u})$ is well known, while that of $r(\mathbf{x};\mathbf{u})$ requires a large number of analyses. For example, when $c(\mathbf{x}; \mathbf{u})$ is failure stress and $r(\mathbf{x}; \mathbf{u})$ is the maximum stress of an aircraft structure, the probabilistic distribution of $c(\mathbf{x}; \mathbf{u})$ is already characterized by Federal Aviation Administration requirement. However, the probabilistic distribution of $r(\mathbf{x}; \mathbf{u})$ requires repeated computational simulations, such as finite element analysis.

Since the performance function depends on two random variables, $c(\mathbf{x};\mathbf{u})$ and $r(\mathbf{x};\mathbf{u})$, the safety of the system can be estimated using a probability of failure, defined as

$$P_f = \Pr[g(\mathbf{x};\mathbf{u}) \le 0] = \int_{-\infty}^{\infty} F_C(\xi)\, f_R(\xi) d\xi \tag{2-2}$$

In the above equation, $F_C(\xi)$ is the cumulative distribution function (CDF) of capacity, and $f_R(\xi)$ is the probability density function (PDF) of response. The above integral can be evaluated using analytical integration, Monte Carlo simulation (MCS), or first-/second-order reliability method (FORM/SORM), among others. Smarslok *et al*. [18] presented a separable MCS, which is much more accurate than the traditional MCS when the performance can be separable as in Eq. 2-1.

It is clear from Eq. 2-2 that accurate estimation of probability of failure requires accurate assessment of the probability distributions of both the response and capacity. When the capacity is the failure stress, the FAA requires aircraft builders to perform characterization tests in order to construct a statistical model, and then to select the allowable failure stress (A-basis or B-basis value) based on this model. Hence, the CDF of capacity is often reasonably well characterized. On the other hand, the PDF of the response is poorly known, because it depends on the accuracy of various factors, such as material properties, operating conditions, mathematical models, and manufacturing variability. The key idea of this research is to express P_f in Eq. 2-2 using a characteristic value of the response, and approximate the change of P_f in terms of the change of this characteristic value.

The calculation of P_f in Eq. 2-2 can be simplified by using the information of $F_C(\xi)$. From the Intermediate Value Theorem [19], there exist r^* such that Eq. 2-2 can be re-written as

$$P_f = F_C(r^*)\int_{-\infty}^{\infty} f_R(\xi)\, d\xi = F_C(r^*) \qquad (2\text{-}3)$$

In the above equation, the second equality is obtained from the fact that the integral of $f_R(\xi)$ is one. Equation 2-3 states that the effect of (the poorly characterized) probability distribution of the response can be boiled down to a single characteristic response, r^*. When the probability of

failure is given, the characteristic response can be calculated using the inverse transformation of $F_C(r^*)$, as

$$r^* = F_C^{-1}(P_f) \tag{2-4}$$

When design variables are changed during optimization, it is possible that the distributions of both capacity and response may be changed. For the simplicity of presentation, we consider the case that the distribution of the capacity remains unchanged. We assume that the design change only affects the mean value of the response; i.e., the standard deviation remains constant. This assumption is reasonable if the design perturbation is small. In such a case, redesign changes the mean value of response from $\bar{r} = r(\mu_X; u)$ to $\bar{r}(1+\Delta)$, where $r(\mu_X; u)$ is the value of response evaluated at the mean value of the input random variables. The variable Δ represents the relative change in response according to design change. At this point, Δ is unknown. Figure 2-1 illustrates the change in response distribution, along with the distribution of capacity.

In this research, we start the probabilistic design from a known deterministic optimum. This is an important aspect of the approximate probabilistic optimization. Since the deterministic optimization uses safety margins to consider the effect of uncertainties, the deterministic optimum design is close to the probabilistic optimum design. This will satisfy the above assumption of small design change. The goal of proposed probabilistic design is then to improve upon the deterministic design by reallocating the safety margins between different components or failure modes.

First, the change in design variables will change the mean of response from $\bar{r}$ to $\bar{r}(1+\Delta)$, while maintaining the same standard deviation. The change in the response distribution will then change the probability of failure according to Eq. 2-2. From Eq. 2-4, the characteristic response will also be changed from r^* to $r^*(1+\Delta^*)$, where Δ^* is the relative change in characteristic

response. Unfortunately, this process requires calculation of the probability of failure at the new design. The novel idea of the proposed approach is to reverse this process by approximating the relation between Δ and Δ* so that the characteristic response at the new design can be calculated without performing reliability analysis. For the moment, let us assume that Δ* can be calculated from given Δ. Then, the probability of failure at the new design can be calculated from

$$P_f^{\text{new}} = F_C\left(r^*(1+\Delta^*)\right) \tag{2-5}$$

The above probability of failure will be exact if Δ* is the correct relative change in characteristic response. When Δ* is an approximated one, the probability of failure in the above equation is approximate, and we will denote it P_f^{approx}. The procedure illustrated in Figure 2-2 does not require expensive reliability analysis. It is enough to analytically evaluate the value of the CDF at the perturbed characteristic response.

Correction Factor

The key idea of the proposed approximate probability distribution is that the new characteristic response can be approximated without recourse to the expensive reliability analysis. The simplest approximation, used in this research, is that the relative change in the characteristic response, Δ* is proportional to the relative change in response, Δ as

$$\Delta^* = k\Delta \tag{2-6}$$

where k is a proportional constant that depends on how the redesign affects the stress distribution. In fact, it is the sensitivity of the characteristic response change with respect to the response change. We call it a *correction factor*. The above assumption in linearity is reasonable when Δ is relatively small.

Probabilistic optimization can be viewed as risk allocation between different failure modes or different structural members. This allocation requires the sensitivity of failure probability with respect to design variables. In the proposed approximate probabilistic optimization, this sensitivity information is presented in the correction factor.

We will demonstrate that a linear relationship between Δ and Δ^* works well given the assumption of translating the stress distribution, especially when the design change is relatively small. We consider a lognormally distributed capacity with mean value of $\mu_C = 100$ and coefficient of variation of 8%, and normally distributed response with coefficient of variation of 20%. From Eq. 2-2, the mean value of the response is chosen to be $\mu_R = 42.49$ so that the probability of failure becomes $P_f = 10^{-7}$. For a given small value of Δ, a new probability of failure P_f^{new} is calculated from Eq. 2-2 with the mean of the response being $\mu_R(1+\Delta)$. The relative change in characteristic response Δ^* is then obtained from Eq. 2-4 with P_f^{new}. Figure 2-3 shows the relation between Δ and Δ^*. We can see that the linearity assumption is quite accurate over the range of $-10\% \leq \Delta \leq 10\%$. The slope will be the correction factor *k*. Figure 2-4 shows the effect of the Δ approximation on the probability of failure. In practice, the correction factor can be calculated using a finite difference method, which requires at least two reliability calculations. We will describe the procedure using a forward finite difference method, but other method can also be used in a similar way. Let $\Delta_o = 0.0$ corresponds to the current design, and $\Delta_p = 0.05$ to the perturbed design. The correction factor can be calculated either using FORM or MSC. We will explain both cases.

Using FORM

First, the probability of failure, P_f, at the current design is calculated from First-Order Reliability Method (FORM) with the performance function in Eq. 2-1. If the response is perturbed by Δ_p, Eq. 2-1 becomes

$$g_p(\mathbf{x};\mathbf{u}) = c(\mathbf{x};\mathbf{u}) - r(\mathbf{x};\mathbf{u})(1+\Delta_p) \tag{2-7}$$

Using the above equation, reliability analysis is performed to calculated the perturbed probability of failure, P_f^p. It is noted that it is unnecessary to change design variable, $\mathbf{u}$, because we directly perturb the output response. Thus, the computational cost of reliability analysis using Eq. 2-7 can be reduced significantly. Next, the characteristic responses are calculated from Eq. 2-4, as

$$\begin{aligned} r^* &= F_C^{-1}(P_f) \\ r_p^* &= F_C^{-1}(P_f^p) = r^*(1+\Delta^*) \end{aligned} \tag{2-8}$$

By comparing two terms in the above equation, the relative change in the characteristic response can be obtained as

$$\Delta^* = \frac{r_p^*}{r^*} - 1 \tag{2-9}$$

Then, the correction factor can be obtained from

$$k = \frac{\Delta^*}{\Delta} \tag{2-10}$$

Using MCS

When MCS is employed, we generate *N* samples of response $r_i = r(x_i;u), i = 1,...,N,$ at the current design. In view of Eq. 2-2, the probabilities of failure at the current and perturbed design can be calculated from

$$P_f = \frac{1}{N}\sum_{i=1}^{N} F_C(r_i) \tag{2-11}$$

$$P_f^p = \frac{1}{N}\sum_{i=1}^{N} F_C\left(r_i(1+\Delta)\right) \tag{2-12}$$

The remaining procedure is identical to that of FORM. Even if Eq. 2-11 and Eq. 2-12 are two different MCS, they can be combined into one because the same sample, r_i, will be used.

Approximate Probabilistic Optimization

The proposed approximate probabilistic optimization is composed of two stages: (1) correction factor k and initial probability of failure P_f are calculated from reliability analysis, and (2) a deterministic optimization problem is solved using the approximate probability of failure from Eq. 2-5. The first stage is computationally expensive, while the second stage is nothing but a semi-deterministic optimization. We will explain the approximate probabilistic optimization procedure, as follows.

1. Perform deterministic optimization with safety margin. The probabilistic design starts from the deterministic optimum design; i.e., initial design $\mathbf{u}_0 = \mathbf{u}_{\text{det}}$ and cost function $W_0 = W_{\text{det}}$. Calculate the initial probability of failure, $P_f = P_f^{\text{det}}$ at $\mathbf{u}_0$.

2. At the current design, $\mathbf{u}_0$, calculate deterministic value of response, $r_0 = r(\mu_{\mathbf{X}}; \mathbf{u}_0)$, using the mean value of input random variables.

3. Calculate the characteristic response, r_0^*, using the inverse CDF of the $P_f{}^{\text{p}}$, and the mean and c.o.v of the response.

4. Calculate the correction factor, k, using the procedure in the previous section.

5. Obtain optimum design $\mathbf{u}_{\text{opt}}$ and optimum objective function W_{opt} by solving the following optimization problem:

$$\begin{aligned} &\min_{\mathbf{u}} \; W(\mu_{\mathbf{X}}, \mathbf{u}) \\ &\text{s.t.} \;\; P_f{}^{\text{approx}} \le P_f^{\text{det}} \end{aligned} \tag{2-13}$$

Where

$$r = r(\mu_{\mathbf{X}}; \mathbf{u}) \tag{2-14}$$

$$\Delta = \frac{r}{r_0} - 1 \tag{2-15}$$

$$\Delta^* = k\,\Delta \tag{2-16}$$

$$r^* = F_C^{-1}(P_f) \tag{2-17}$$

$$P_f^{\text{approx}} = F_C\left[r^*\left(1+\Delta^*\right)\right] \tag{2-18}$$

6. Calculate the actual probability of failure, P_f, at $\mathbf{u}_{\text{opt}}$.

7. Check convergence: $\left|P_f^{\text{approx}} - P_f\right| \le \varepsilon$. If it converged, stop the process. Otherwise, set $\mathbf{u}_0 = \mathbf{u}_{\text{opt}}$ and go to Step 2 and continue.

The above semi-deterministic optimization process uses exact distribution of the capacity (F_C) and an approximate distribution of response (MCS or FORM). Due to this aspect, we call it Exact-Capacity-Approximate-Response Distribution (ECARD) method. The accuracy of ECARD to locate the true optimum depends on the magnitudes of errors involved in the approximations. As shown in Figure 2-3 and Figure 2-4, the approximation is accurate if changes of the response due to redesign are small. In addition, the accuracy in estimating the correction factor k affects the convergence rate of the proposed method. The result may be somewhat sub-optimal because of the convergence condition and the approximate nature of the sensitivity of probability of failure. This issue will be discussed in detail in the following section.

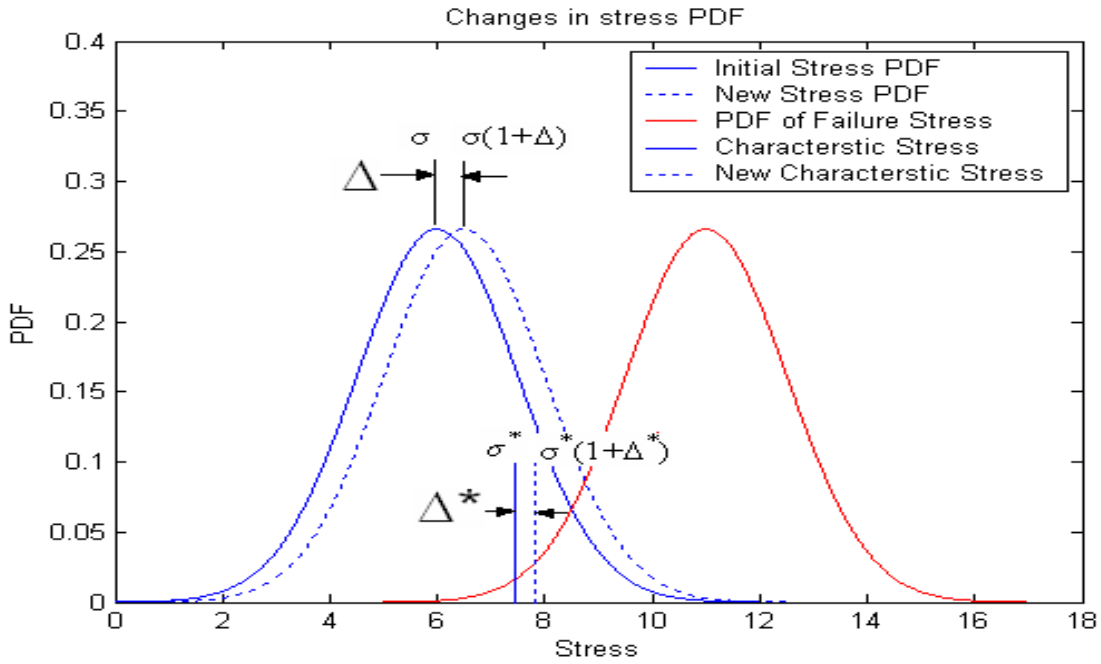

Figure 2-1. Distributions of response before and after redesign.

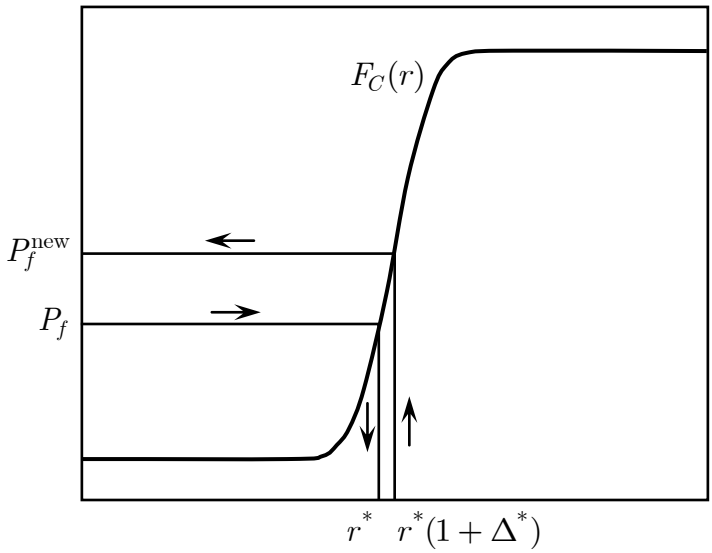

Figure 2-2. Calculation of the probability of failure at new design.

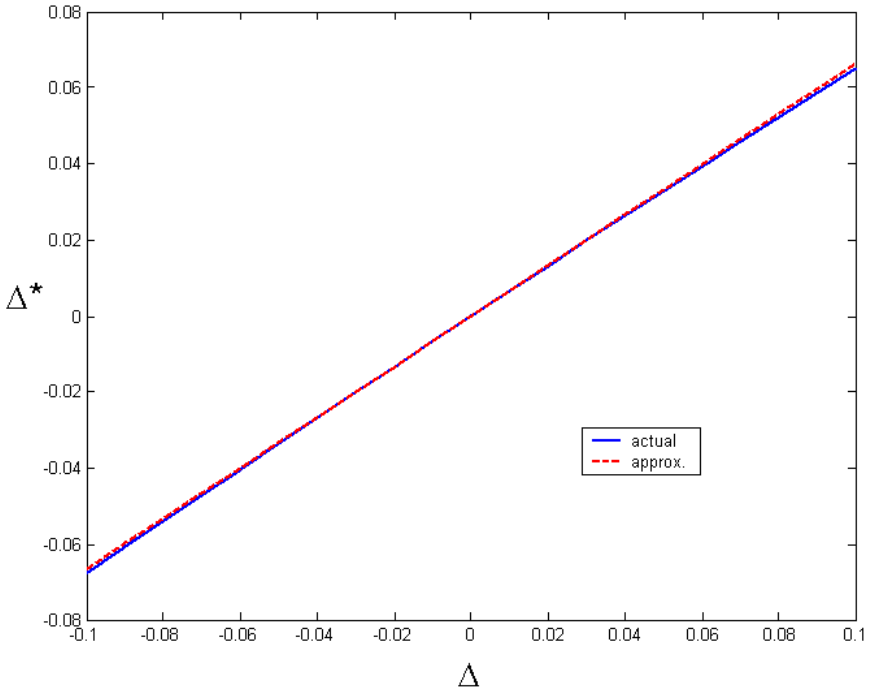

Figure 2-3. Calculation of the probability of failure at new design

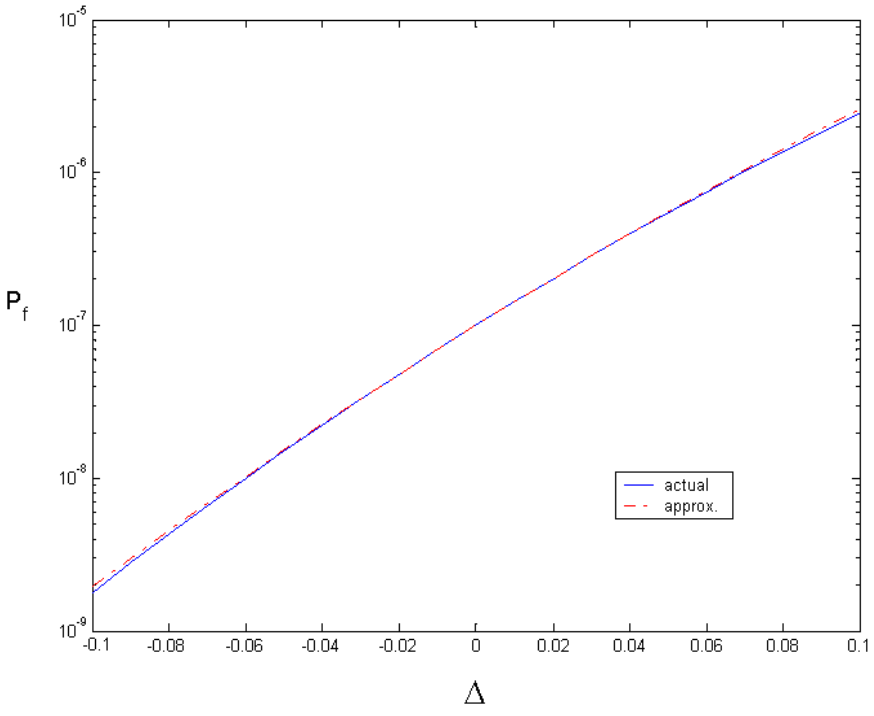

Figure 2-4. Calculation of the probability of failure at new design

CHAPTER 3
ANALYTICAL EXAMPLE: APPLICATION OF ECARD TO A TEN-BAR TRUSS

Introduction

The first demonstration example is a ten-bar truss problem as shown in Figure 3-1. This example will demonstrate risk allocation between the different truss members. First, a brief description of the problem will be given. Then, a deterministic optimization of the problem will be presented followed by the probability of failure calculation using Monte Carlo simulations. Finally, the probabilistic and ECARD optimizations will be performed, and the efficiency and accuracy of the ECARD method will be discussed.

Problem Description

The problem description for the ten-bar truss example was taken from Haftka and Gurdal [20] (page 237). The truss structure is under two loads, P_1 and P_2. The design objective is to minimize the total weight of the truss, W, by varying the cross-sectional areas, A_i, of the members while satisfying minimum gage constraints and allowable stress constraints. Input data for the truss is listed in Table 3-1. Member 9 was assigned a higher failure stress value in order to make the fully stressed design non-optimal. Aircraft design often uses a knockdown factor, K_{dc}, in order to conservatively estimate failure stress using A-basis or B-Basis methods. The A-basis (or B-basis) failure stress is the value of a failure stress exceeded by 99% (or 90% for B-basis) of the population with 95% confidence. In the conservative estimation, the allowable stress of a member is related to the mean value of the failure stress through the following equation:

$$\sigma_{\text{allowable}} = K_{dc}\mu_{\sigma_f} \tag{3-1}$$

In the deterministic design process, the knockdown factor is a way of considering the uncertainty in the failure stress.

Deterministic Optimization

Using the safety factor and knockdown factor, the deterministic optimization problem can be formulated as

$$\begin{aligned} &\min_{A_i} \; W = \sum_{i=1}^{10} \rho L_i A_i \\ &\text{s.t.} \;\; \frac{N_i(S_F P_1, S_F P_2, \mathbf{A})}{A_i} = \sigma_i \le (\sigma_{\text{allowable}})_i, \\ &0.1 \le A_i \end{aligned} \tag{3-2}$$

where L_i, N_i, and A_i are, respectively, the length, member force, and cross-sectional area of element i. $\mathbf{A}$ is the vector of cross-sectional areas, σ_i and $(\sigma_{allowable})_i$ are the stress and allowable stress of an element, respectively. For this example, σ_i, corresponds to the response while $(\sigma_{allowable})_i$ to the capacity, and the loads are multiplied by a safety factor in order to consider various uncertainties involved in the truss parameters, applied load, and computational errors. The analytical solution for the member forces are given in the Appendix. The above optimization problem is solved using the "fmincon" function in MATLAB. The problem converged in 7 iterations with 97 function evaluations. Table 3-2 lists the results of the deterministic optimization. Note that elements 2, 5, and 6 cross-sectional areas reach minimum gage while element 5 is a zero force member. At optimum design, stresses in all members except for Member 5 and 9 are at the allowable stress.

Probability of Failure Calculation Using MCS

In this section, the probability of failure of the truss at the deterministic optimum design is evaluated using Monte Carlo Simulation (MCS). There are two purposes in calculating the probability of failure. First, it can evaluate the level of safety of the deterministic optimum design. The effects of the knockdown factor and the factor of safety are evaluated in terms of the probability of failure. Second, it can be used for the design criterion in the probabilistic

optimization. In the calculation of the probability of failure, the factor of safety and the knockdown factor will not be considered. Instead, uncertainties related to errors and variability in material properties, manufacturing tolerances, and applied loads will be considered in calculating the probability of failure.

There are many uncertainties involved in the design of the ten-bar truss, such as variability from material properties, loads, manufacturing, and errors from numerical calculation and modeling. Failure of an element is predicted to occur when the stress in an element is greater than its failure stress. Knowing this, the performance function can be written as

$$g = \left(\sigma_f\right)_{\text{true}} - \sigma_{\text{true}} \tag{3-3}$$

where the subscript 'true' stands for the true value of the relevant quantity, which is different from its calculated (or predicted) value due to errors. Adding these errors, the equation can be rewritten as

$$g = \left(1 - e_f\right)\sigma_f - \left(1 + e_\sigma\right)\sigma \tag{3-4}$$

Here, e_f is the error in failure prediction, σ_f is the predicted failure stress, e_σ is the error in stress calculation, and σ is the calculated stress. The errors were formulated to where positive errors correspond to a conservative design. Therefore, the error in calculated stress is positive, while the error in predicted failure stress is negative. Even though the stress calculation is exact for the ten-bar truss, the error, e_σ, was introduced to consider the analysis of a more complex structure where the stresses are calculated from numerical methods. The calculated stress can be written in the following form

$$\sigma = \sigma_{\text{FEA}}\left[\left(1 + e_{P1}\right)P_1, \left(1 + e_{P2}\right)P_2, \left(1 + \mathbf{e}_\mathbf{A}\right)\mathbf{A}\right] \tag{3-5}$$

where σ_{FEA} stands for calculated stresses using FEA, e_{P1} and e_{P2} are errors in loads P_1 and P_2, and $\mathbf{e}_\text{A}$ is the vector of errors (tolerances) corresponding to ten cross-sectional areas. By

substituting Eq. 3-5 into Eq. 3-4, the performance function can now be rearranged in separable form (i.e., in a form that allows the use of separable MCS) for each element as

$$g_i = (\sigma_f)_i - \frac{(1+e_\sigma)}{(1-e_f)}\,\sigma_{\text{FEA}}\left[(1+e_{P1})P_1,(1+e_{P2})P_2,(1+\mathbf{e}_\mathbf{A})\mathbf{A}\right]_i \equiv c_i - r_i \qquad (3\text{-}6)$$

where c_i and r_i are respectively, the capacity and response. Beside errors, variabilities are introduced into the performance function through random variables σ_f, P_1, P_2, and A. The probabilistic parameters of errors and variabilities and their distribution types are listed in Table 3-3. The probabilities of failure were calculated using separable MCS, which requires smaller number of simulations to achieve the same accuracy as crude MCS [17]. After calculating the probabilities of failure for each element, the total probability of failure of the system can be approximated as

$$P_{FS} = \sum_{i=1}^{10}(P_f)_i \qquad (3\text{-}7)$$

where P_{FS} is the system probability of failure. Calculating the probability failure in this form is Ditlevesen's first-order upper bound; therefore the system probability of failure is estimated conservatively. Using separable MCS with 10^6 samples, the probabilities of failure for each element and the system are listed in Table 3-4. The results show that members 2, 6, and 10's probability of failure contributes to 80% of the system probability of failure.

In the deterministic design process, the uncertainty in the system is considered using safety measures, such as knockdown factor and the factor of safety. However, as is clear form Table 3-4, the effects of these safety measures are not evenly distributed between members. It appears that members 2, 6, and 10 are very sensitive to these safety measures, while other members are not. They are either at minimum gage or close to it, and yet, their probabilities of failure are relatively high compared to the other members. Thus, it is possible to move some of the weight

from non-sensitive members to the sensitive ones so that the system probability of failure can be reduced further while maintaining the total weight of the truss. Or, it is also possible to reduce the weight of the truss while maintaining the same level of system probability of failure. The latter possibility will be investigated in the probabilistic optimization.

Probabilistic Optimization

Starting from the deterministic design, the probabilistic optimization problem can be formulated such that the weight of the structure is minimized, while maintaining the same level of system probability of failure with that of the deterministic optimum design. Thus, we have

$$\begin{aligned} &\min_{A_i} \; W = \sum_{i=1}^{10} \rho L_i A_i \\ &\text{s.t.} \quad P_{FS} \le P_{FS}^{\text{det}} \end{aligned} \tag{3-8}$$

Results of the probabilistic optimization are shown in Table 3-5. A total of 10^5 samples are used for MCS. The optimization converged after 59 iterations and 728 reliability assessments. The relatively large number of reliability assessments is due to the fact that the problem has ten design variables. At each iteration, the optimization algorithm calculates sensitivity using finite different method. On the other hand, the proposed ECARD method perturbs the response directly. Thus, ECARD will be efficient when the number of response is smaller than that of design variables.

The overall optimization took about 125 hours using a Dell desktop computer. In order to remove instability related to random samples, a set of input random variables are generated and repeatedly used during the optimization. Overall weight is reduced by 6% (90.47 lbs) while maintaining the same system probability of failure as that of the deterministic optimum design. This reduction is achieved by reallocating the risk from the higher risk members (2, 6, and 10) to the lower risk members. The probabilistic optimization slightly increased the cross-sectional

areas of members 2, 6, and 10, and decreased the cross-sectional areas of the other members. While the remaining member's probabilities of failure increased slightly, members 2, 6, and 10 were reduced by an order of magnitude. This risk allocation can be achieved when the sensitivities of probability of failure and weight with respect to design variables are available. In the probabilistic optimization, these sensitivities are calculated using the finite difference method. That explains the 728 reliability assessments during the optimization. In the following section, the same optimization problem will be solved using the ECARD method, which requires a smaller amount of reliability assessments, and yet the sensitivity information can be obtained in the approximate sense.

Approximate Probabilistic Optimization Using ECARD

In the approximate probabilistic design, the same optimization problem is used except that the approximate probability of failure is used. Thus, the optimization problem can be written as

$$\begin{aligned} &\min_{A_i} \; W = \sum_{i=1}^{10} \rho L_i A_i \\ &\text{s.t.} \quad P_{FS}^{\text{approx}} \le P_{FS}^{\text{det}} \end{aligned} \tag{3-9}$$

where the approximate system probability of failure is the sum of each members contributions. Since there are ten members, ten characteristic responses and correction factors are calculated before the ECARD optimization. This calculation is equivalent to assessing the probability of failure twice. Then, the above optimization is deterministic because the approximate probability of failure can be evaluated without MCS. Since the approximation in the probability of failure is not accurate, the above ECARD optimization is repeated until the convergence criterion, as stated in Chapter 2, is satisfied.

The accuracy of the characteristic response, which depends on the number of MCS samples, affects the number of iterations needed to reach an accurate optimum. A low number of

samples may appear to reduce computational costs, but actually it reduces the confidence in the probability of failure calculation resulting in an increased number of iterations to reach the accurate optimum. The number of MCS samples must be chosen accordingly for each problem.

The results of the ECARD optimization are displayed in Table 3-6. Using 10^5 MCS samples, the ECARD optimization needed only four iterations and 8 reliability assessments to reach close to the probabilistic optimum. This is a significant reduction from the 728 reliability assessments of the probabilistic optimization. The weight difference when comparing the fourth iteration to the third is 0.03%, while the approximate system probability of failure equals the deterministic system probability of failure. In addition, the errors in the member approximate probability of failure calculations are less than 2%. Since, the probability of failure for member nine is very small, its probability of failure error is not accurate and the error is ignored. As expected the ECARD optimization allocates the risk between members. The cross-sectional areas of the smaller members increased while they decreased in the largest members.

Table 3-1. Parameters for the ten-bar truss problem

Parameters	Values
Dimension, b	360 inches
Safety factor, S_F	1.5
Load, P_1	66.67 kips
Load, P_2	66.67 kips
Knockdown factor, K_{dc}	0.87
Density, r	0.1 lb/in^3
Modulus of elasticity, E	10^4 ksi
Allowable stress, $\sigma_{\text{allowable}}$	25 ksi*
Minimum gage	0.1 in^2

*for Element 9, allowable stress is 75 ksi

Table 3-2. Results of deterministic optimization of the ten-bar truss problem

Element	A_i^{det} (in)	W_i (lb)	Stress (ksi)
1	7.900	284.400	25.0
2	0.100	3.600	25.0
3	8.100	291.600	-25.0
4	3.900	140.400	-25.0
5	0.100	3.600	0.0
6	0.100	3.600	25.0
7	5.798	295.200	25.0
8	5.515	280.800	-25.0
9	3.677	187.200	37.5
10	0.141	7.200	-25.0
Total	---	1497.600	---

Table 3-3. Probabilistic distribution types, parameters of errors and variabilities in the ten-bar truss problem

Uncertainties	Distribution type	Mean	Scatter
Errors			
e_σ	Uniform	0	± 5%
e_{P1}	Uniform	0	± 10%
e_{P2}	Uniform	0	± 10%
$e_{\mathbf{A}}$ (10×1 vector)	Uniform	0	± 3%
e_f	Uniform	0	± 20%
Variability			
P_1, P_2	Extreme type I	66.67 kips	10% c.o.v.
A (10×1 vector)	Uniform	**A** (10×1 vector)	4% bounds
σ_f	Lognormal	$25/k_{dc}$ ksi or $75/k_{dc}$ ksi	8% c.o.v.

Table 3-4. Probabilities of failure of the deterministic optimum areas

Element	P_f^{det}
1	2.13E-03
2	1.06E-02
3	4.80E-04
4	2.19E-03
5	4.04E-04
6	1.07E-02
7	1.69E-03
8	1.89E-03
9	5.47E-13
10	1.07E-02
Total	4.08E-02

Table 3-5. Results of the probabilistic optimization of the ten-bar truss

Elements	A_i^{det} (in)	A_i	$(P_f^{det})_i$	$(P_f)_i$
1	7.9	7.192	2.13E-03	5.88E-03
2	0.1	0.3243	1.06E-02	3.07E-03
3	8.1	7.162	4.80E-04	8.26E-03
4	3.9	3.701	2.19E-03	2.15E-03
5	0.1	0.4512	4.04E-04	3.18E-05
6	0.1	0.3337	1.07E-02	2.14E-03
7	5.798	5.1697	1.69E-03	1.02E-02
8	5.515	4.9782	1.89E-03	3.75E-03
9	3.677	3.5069	5.47E-13	4.70E-13
10	0.141	0.4325	1.07E-02	5.46E-03
Total	1497.6 lbs	1407.13 lbs	4.08E-02	4.08E-02

Table 3-6. Results of the ECARD optimization

Element	Determ. Des.	Iter 1	Iter 2	Iter 3	Iter 4
		AREAS (in^2)			
1	7.9000	7.4487	7.4787	7.4841	7.4849
2	0.1000	0.1000	0.1000	0.1000	0.1000
3	8.1000	7.0752	7.0406	7.0401	7.0402
4	3.9000	3.9382	3.9666	3.9710	3.9716
5	0.1000	0.1000	0.1000	0.1000	0.1000
6	0.1000	0.1000	0.1000	0.1000	0.1000
7	5.7980	5.0457	5.0440	5.0442	5.0441
8	5.5150	5.3538	5.3873	5.3941	5.3951
9	3.6770	3.8416	3.9657	3.9873	3.9908
10	0.1410	0.1314	0.1310	0.1309	0.1309
Weight (lb)	1497.60	1407.16	1415.94	1417.71	1418.00
		MEAN STRESSES (ksi)			
1	16.6667	17.7656	17.7047	17.6934	17.6918
2	16.6667	14.479	14.0059	13.9276	13.9147
3	-16.6667	-18.9868	-19.0693	-19.0688	-19.0684
4	-16.6667	-16.5606	-16.4537	-16.4378	-16.4354
5	0	4.462	4.7514	4.7913	4.7977
6	16.6667	14.479	14.0059	13.9276	13.9147
7	16.6667	18.966	18.951	18.9472	18.9468
8	-16.6667	-17.3456	-17.2576	-17.2391	-17.2363
9	25	24.0093	23.2747	23.1515	23.1313
10	-16.6667	-15.5797	-15.1199	-15.0471	-15.0354

Table 3-7. Results of the ECARD optimization

Element	Determ. Des.	Iter 1	Iter 2	Iter 3	Iter 4
APPROXIMATE P_F					
1	2.13E-03	5.65E-03	5.26E-03	5.21E-03	5.20E-03
2	1.06E-02	2.16E-03	2.11E-03	2.10E-03	2.10E-03
3	4.80E-04	7.44E-03	7.51E-03	7.51E-03	7.50E-03
4	2.19E-03	1.97E-03	1.77E-03	1.74E-03	1.74E-03
5	4.04E-04	4.04E-04	1.72E-03	1.86E-03	1.88E-03
6	1.07E-02	2.17E-03	2.09E-03	2.09E-03	2.09E-03
7	1.69E-03	1.23E-02	1.20E-02	1.20E-02	1.20E-02
8	1.89E-03	3.59E-03	3.22E-03	3.17E-03	3.16E-03
9	5.47E-13	3.09E-14	2.50E-15	1.67E-15	6.66E-16
10	1.07E-02	5.17E-03	5.21E-03	5.22E-03	5.23E-03
SYSTEM	4.08E-02	4.08E-02	4.08E-02	4.08E-02	4.08E-02
ACTUAL P_F					
1	2.13E-03	5.53E-03	5.26E-03	5.21E-03	5.20E-03
2	1.06E-02	3.09E-03	2.25E-03	2.13E-03	2.11E-03
3	4.80E-04	6.95E-03	7.51E-03	7.51E-03	7.50E-03
4	2.19E-03	1.96E-03	1.77E-03	1.74E-03	1.74E-03
5	4.04E-04	1.72E-03	1.86E-03	1.88E-03	1.88E-03
6	1.07E-02	3.09E-03	2.23E-03	2.11E-03	2.09E-03
7	1.69E-03	1.21E-02	1.20E-02	1.20E-02	1.20E-02
8	1.89E-03	3.49E-03	3.22E-03	3.17E-03	3.16E-03
9	5.47E-13	2.77E-14	2.44E-15	1.59E-15	1.48E-15
10	1.07E-02	7.14E-03	5.50E-03	5.27E-03	5.24E-03
SYSTEM	4.08E-02	4.51E-02	4.16E-02	4.10E-02	4.08E-02

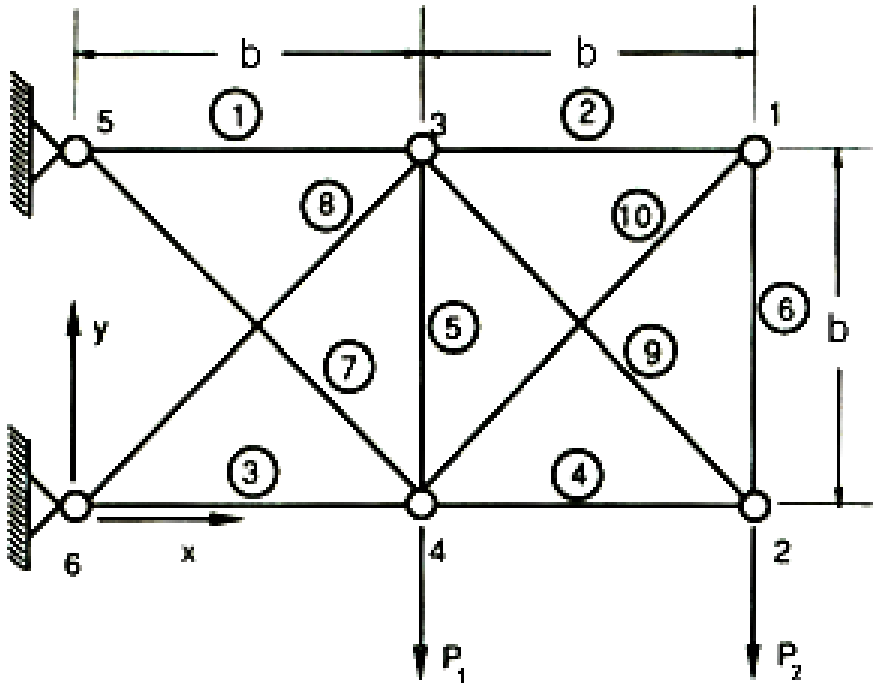

Figure 3-1. Geometry and loadings of the ten-bar truss

CHAPTER 4
PRACTICAL EXAMPLE: APPLICATION OF ECARD TO A WINGBOX MODEL

Introduction

The second demonstration example is the wingbox model problem. This example will demonstrate the risk allocation between different failure modes of stress and displacement while minimizing the total weight of the wingbox. Publically available information was used to model the wingbox as a Boeing 767 wing in a 2.5 g dive. First, a description of the problem will be given which will cover model geometry, and loading calculations. Then, a deterministic optimization of the problem will be presented followed by the probability of failure calculation using Monte Carlo simulations. Finally, the ECARD optimization will be performed, and the efficiency and accuracy of the ECARD method will be discussed.

Problem Description

Geometry

The geometry of the wingbox was modeled using the open source Boeing 767 wing schematics shown in Figures 4-1 and 4-2. The root dimensions have a width of 170 inches with a height of 50 inch. The tip dimensions are 20 inches wide, 10 inches tall. The skin thickness at the root is 1.0 inches and decreases in steps linearly to 0.1 inches at the tip of the wing. The wing is 745 inches long from root to tip.

The wingbox is modeled using ANSYS Parametric Design Language (APDL) and analyzed using ANSYS Finite Element Analysis software. Since the APDL is a parametric language, it can generate finite element models with different design values. The APDL code consists of a set of commands that instructs ANSYS to build the model, add the loading and boundary conditions, and conduct the FEA analysis. The design variables of the model are the skin thicknesses at the root and midpoint of the wingbox. The tip thickness is fixed to 0.1 in.

The thickness varies linearly between the root and midpoint, and between the midpoint and the tip. Figure 4-3 shows the ANSYS model of the wingbox.

The model contains a total of 5,105 nodes, 5,652 elements and was meshed using SHELL 63 Elastic Shell elements. The element contains four nodes, four thicknesses, and orthotropic material properties. It also has six degrees of freedom at each node, translations in the x, y, and z directions and rotations about the nodal x, y, and z axes. The boundary conditions are that all nodes at the root of the wing are constrained in all directions. Figure 4-4 shows the meshed wingbox model.

The material properties of the model are based on 7150-T77 aluminum, which were taken from Metallic Materials Properties Development and Standardization (MMPDS) [21]. These material properties are listed in Table 4-1.

Loading Calculations

The stresses and deflections of the wingbox model are calculated using mechanics of materials methods. Determination of these stresses and deflections requires simplifying assumptions on the geometry of the structure. Without losing generality, the following simplifying assumptions have been made:

1. The cross section of the wing is made of thin hollow rectangular box section and the platform is trapezoidal. The wing is modeled as a cantilever beam clamped at its root section and free at its ends.

2. The lift over the surface of the wing area is replaced by a line load (lift per unit length) elliptically distributed over a sweep of a line whose locus of pointes are one-quarter of the chord from leading edge (c/4 line), as seen in Figure 4-5.

Wing lift distribution is directly related to the wing geometry and determines such wing performance characteristics as induced drag, structural weight, and stalling characteristics. The distribution of the aerodynamic lift along the span of a wing is commonly regarded as elliptical

and depends (among other things) on the taper ratio λ. For an elliptical lift distribution shown in Figure 4-6, the lift, *w* on the total span length of both wings, *L* is defined by the equation of an ellipse.

$$\frac{x^2}{(L/2)^2}+\frac{w^2}{w_o^2}=1 \tag{4-1}$$

Where, w_o is the maximum load per unit length at the center of the fuselage ($x = 0$). The value of w_o is determined from the gross weight of the aircraft at landing. For straight and level flight, the total aerodynamic lift is equal to the area of the ellipse and must be equal to the gross weight of the aircraft. Hence, lift per wing is

$$\text{Weight of Airplane x g-force} = \frac{1}{4}\pi w_o L \tag{4-2}$$

Now solving for w_o in Equation 4-2 at 2.5 g,

$$w_o = 3.181 \cdot \frac{W_g}{L} \tag{4-3}$$

where W_g is the aircraft gross weight. The lift per unit length *w* at any section of the wing is, hence, given by

$$w = \frac{2w_o}{L}\sqrt{\left(\frac{L}{2}\right)^2 - x^2} \tag{4-4}$$

The lift distribution varies from 747.21 lbs/in at the root to 0 lbs/in at the wingtip. The plot of the lift distribution is seen in Figure 4-7. The elliptical lift distribution can now be converted into a pressure load, *p* on the wing and the force per unit length, *F* acting on the leading edge of the chord as shown in Figure 4-8. Equilibrium of forces in the vertical direction requires

$$\begin{aligned} Pc + F - w &= 0 \\ Pc + F &= w \end{aligned} \tag{4-5}$$

Equilibrium of the moments about the quarter chord requires

$$-F \cdot \frac{c}{4} + Pc\left(\frac{c}{2} - \frac{c}{4}\right) = 0 \rightarrow F \cdot \frac{c}{4} + Pc \cdot \frac{c}{4} = 0 \qquad (4\text{-}6)$$
$$F = Pc$$

Solving for p, and F from Eq. 4-5 and Eq. 4-6 yields

$$p = \frac{w}{2c} \qquad (4\text{-}7)$$
$$F = \frac{w}{2}$$

Using these equations, the pressure at the root was calculated to be 2.198 lbs/in^2 to 0 lbs/in^2 at the tip, while the force at the leading edge was calculated to be 373.61 lbs/in to 0 lbs/in at the tip. Plot of the pressure and force can be seen in Figures 4-9 and 4-10. Half the distribution obtained from Eq. 4-7 is applied to the top of the model while the other half is applied to the bottom of the model. This was done in order to reduce errors in the FEA analysis of the wingbox model.

Deterministic Optimization

The deterministic optimization problem can be formulated as

$$\begin{aligned} &\min\ W = \sum_{i=1}^{\#elements} \rho V_i \\ &\text{s.t.}\ \ \sigma_i \le (\sigma_{A-basis}), \\ &TipDisplacement \le (TipDisplacement)_{allow} \end{aligned} \qquad (4\text{-}8)$$

where V_i, σ_i and ($\sigma_{A\text{-}basis}$) are the volume, stress and A-basis allowable stress of the material, respectively. The design variables are the skin thicknesses at the root and midpoint of the wingbox. Maximum allowable values for the problem are the A-basis value of 7150-T77 aluminum for stress and 68.2 inches for displacement. In this example, σ_i and the calculated tip displacement corresponds to the response while ($\sigma_{A\text{-}basis}$) and allowable tip displacement to the capacity. The loads are multiplied by a safety factor of 1.5 in order to consider various uncertainties involved in the geometric parameters, applied load, and computational errors. The

above optimization problem is solved using the "fmincon" function in MATLAB. The MATLAB code will input the initial design variables into ANSYS, which will conduct the analysis. ANSYS then sends the maximum von Mises element stress, tip displacement data, and total volume of the structure back to MATLAB, which will work to find the design parameters that minimizes the structural weight, while satisfying stress and displacement constraints. The optimization problem converged in 7 iterations with 36 function evaluations. Table 4-2 lists the results of the deterministic optimization. It should be noted that the maximum stress occurs at the root of the wing model. A contour plot of the element stress can be viewed in Figure 4-11.

Probability of Failure Calculation Using MCS

In this section, the probability of failure of the wingbox at the deterministic optimum design is evaluated using Monte Carlo Simulation (MCS). As stated in Chapter 3, the purpose of the probability of failure is to evaluate the level of safety of the deterministic optimum design. It will also be used for the design criterion in the probabilistic optimization. In the calculation of the probability of failure, the factor of safety will not be considered. Instead, uncertainties related to variability in material properties, manufacturing tolerances, and applied loads will be considered in calculating the probability of failure.

Failure of the wingbox is predicted to occur when its maximum von Mises stress and tip displacement is greater than its A-basis failure stress value and allowable displacement. Knowing this, the performance function corresponding to the failure stress mode can be written as

$$g_1 = \left(\sigma_{A-basis}\right) - \sigma_{FEA} \equiv c_1 - r_1 \tag{4-9}$$

where c_1 and r_1 are the capacity and response of g_1. Similarity, the performance function corresponding to the displacement failure mode can be written as

$$g_2 = (TipDisplacement)_{allowable} - (TipDisplacement)_{FEA} \equiv c_2 - r_2 \quad (4\text{-}10)$$

where c_2 and r_2 are the capacity and response of g_2.

Variabilities are introduced into the performance function through random variables $\sigma_{A\text{-}basis}$, $(Tip\ Displacement)_{allowable}$ and a load factor. The means and standard deviations of random variables are listed in Table 4-3. As in the ten-bar truss example, the probabilities of failure were calculated using separable MCS. After calculating the probabilities of failure, the total probability of failure of the system can be approximated as

$$P_F^{\det} = P_{f1} + P_{f2} \quad (4\text{-}11)$$

where P_F is the system probability of failure, P_{f1} is the probability of failure of the stress failure mode, and P_{f2} is the probability of failure of the displacement failure mode. Using separable MCS with 10^6 samples, the probabilities of failure for each element and the system are listed in Table 4-4. The results show that the probability of failure of the displacement failure mode is an about six times larger than the probability of failure of the stress failure mode. Since the stress is a local performance, it depends on the thickness of the root. On the other hand, the displacement is a global performance and its value depends on the thickness of entire wingbox. Thus, it is possible to increase the thickness of the midpoint design variable, which will reduce the probability of failure of the displacement failure mode, while simultaneously decreasing the thickness of root design variable, which will increase the probability of failure of the stress failure mode. This will make it possible to reduce the weight of the wing model while maintaining the same level of system probability of failure.

Approximate Probabilistic Optimization Using ECARD

Starting from the deterministic design, the approximate probabilistic optimization problem can be formulated such that the weight of the structure is minimized, while maintaining the same

system probability of failure with that of the deterministic optimum design. Instead of the actual probability of failure, the approximate probability of failure from ECARD is used. Thus, the optimization problem can be written as

$$\begin{aligned} &\min\ W = \sum_{i=1}^{\#elements} \rho V_i \\ &\text{s.t.}\quad P_F{}^{approx} = P_{f1}{}^{approx} + P_{f2}{}^{approx} \le P_F{}^{\det} \end{aligned} \tag{4-12}$$

where the approximate system probability of failure is the sum of each approximate probability of failure mode. Before the ECARD optimization, a characteristic response and correction factors are calculated for each failure mode. The results of the ECARD optimization are displayed in Table 4-5. Using 10^6 MCS samples, the ECARD optimization needed only two iterations and 4 reliability assessments to reach close to an accurate optimum. Overall weight is reduced by 0.22% (42.7 lbs) while maintaining the same system probability of failure as that of the deterministic optimum design. This reduction is achieved by reallocating the risk from the higher risk displacement failure mode to the lower risk stress failure mode. The ECARD optimization slightly increased the midpoint thickness and decreased the root thickness. This resulted in a similar level of probabilities of failure between the displacement and stress failure modes.

Table 4-1. Material Properties of 7150-T77 Aluminum

7150-T77 Aluminum
Yield Strength = 80.5 ksi A-Basis = 74 ksi B-Basis = 79 ksi

Table 4-2. Results of deterministic optimization of the wingbox model

Root Thickness (in)	Midpoint Thickness (in)	Deterministic Weight (lbs)
0.78226	0.44164	19,174.40

Table 4-3. Variability for Wing Model

Uncertainties	Distribution type	Mean	Standard Deviation	COV
Load Factor	Normal	1	0.1	10%
Failure Stress	Normal	80,500 psi	5072 psi	6.30%
Displacement	Normal	68.2 in	3.41 in	5%

Table 4-4. Probabilities of failure of the deterministic optimum design

P_{f1}	P_{f2}	P_F
5.26E-06	3.17E-05	3.69E-05

Table 4-5. ECARD optimization results

Iteration 1					
	Prob Thickness (in)		Mean Value	Approx Pf	Actual Pf
Root	0.7666	Stress:	50,257 psi	1.110E-05	1.141E-05
Midpoint	0.4533	Displacement:	45.249 in	2.584E-05	2.545E-05
			Total Pf:	3.694E-05	3.687E-05
		Prob Weight:	19132.6 lbs		

Iteration 2					
	Prob Thickness (in)		Mean Value	Approx Pf	Actual Pf
Root	0.7668	Stress:	50,246 psi	1.131E-05	1.130E-05
Midpoint	0.4531	Displacement:	45.255 in	2.563E-05	2.564E-05
			Total Pf:	3.694E-05	3.694E-05
		Prob Weight:	19131.7 lbs		

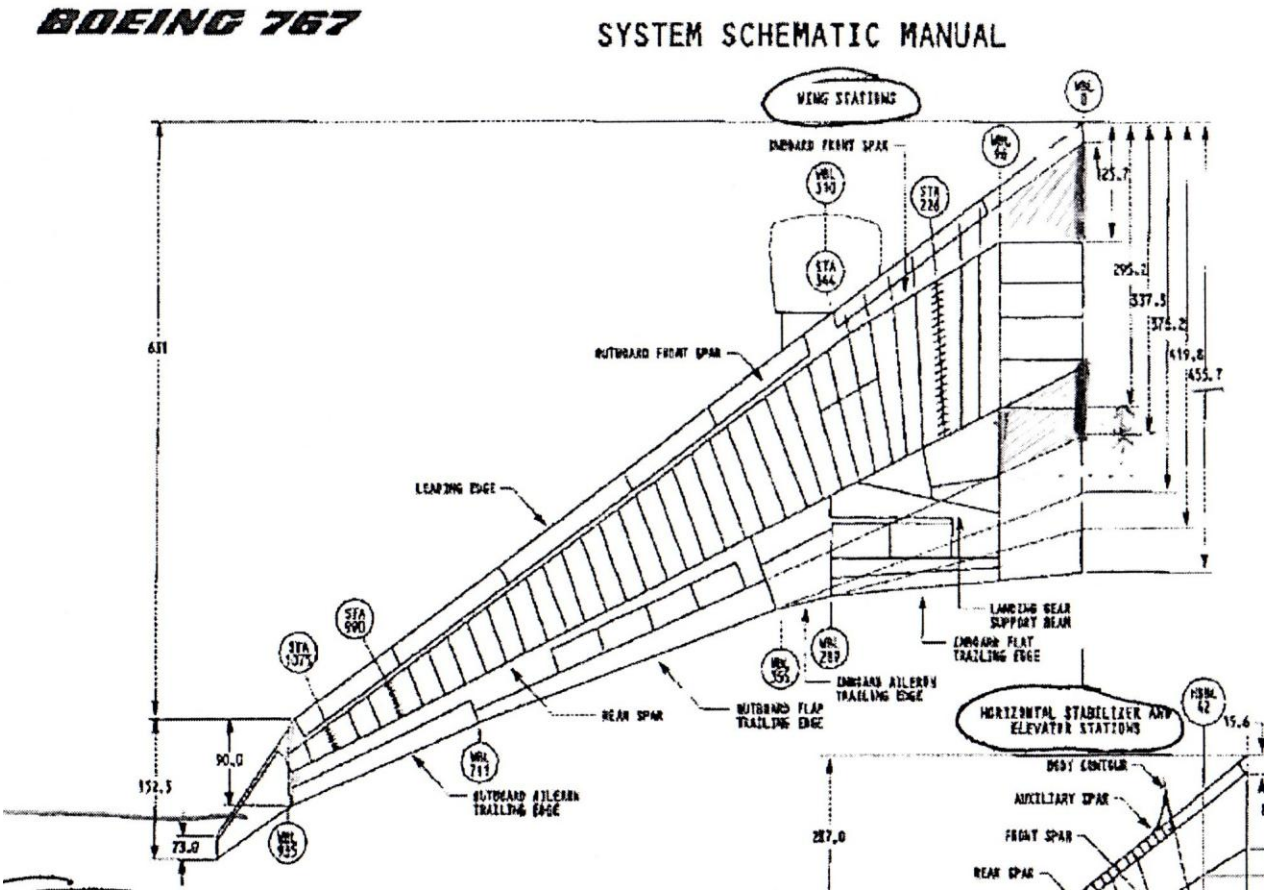

Figure 4-1. Boeing 767 wing dimensions

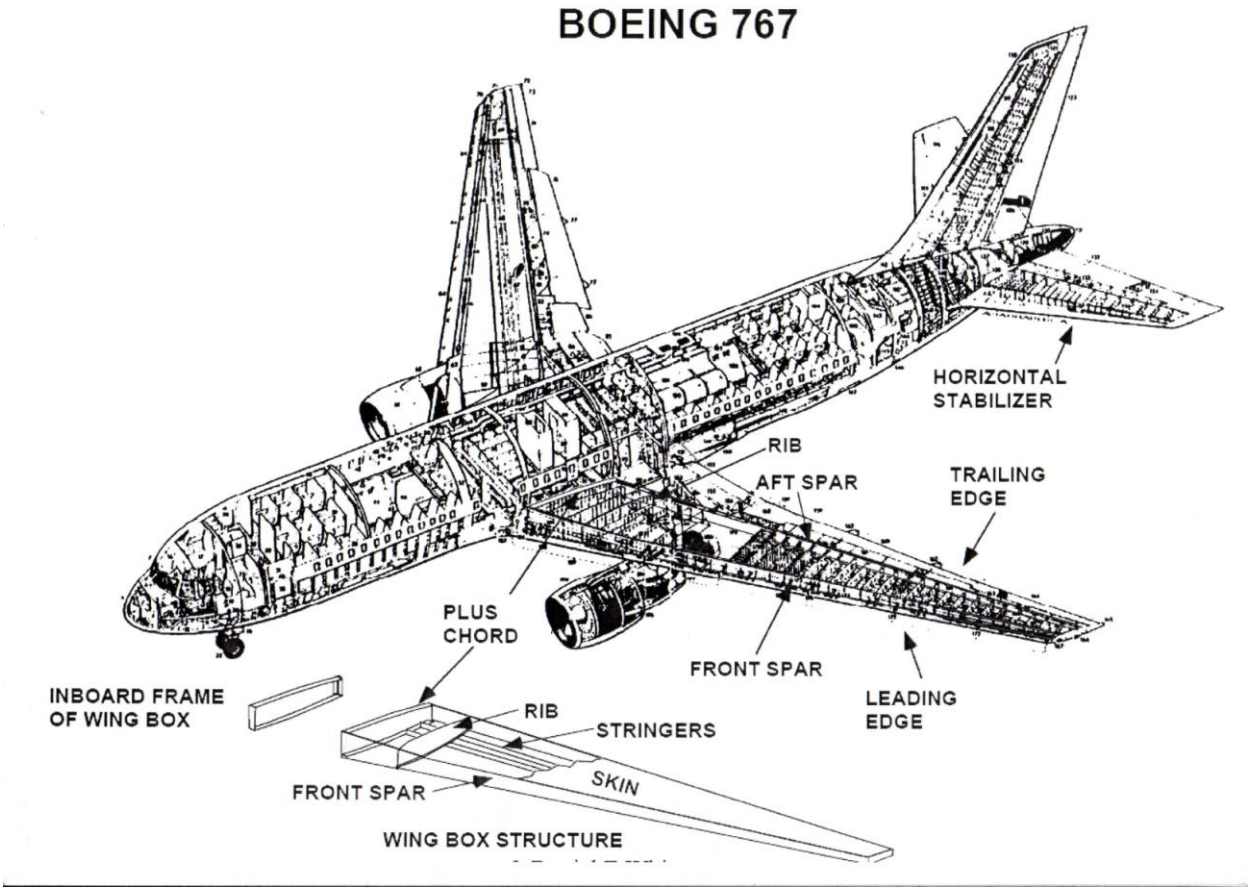

Figure 4-2. Boeing 767 internal schematic

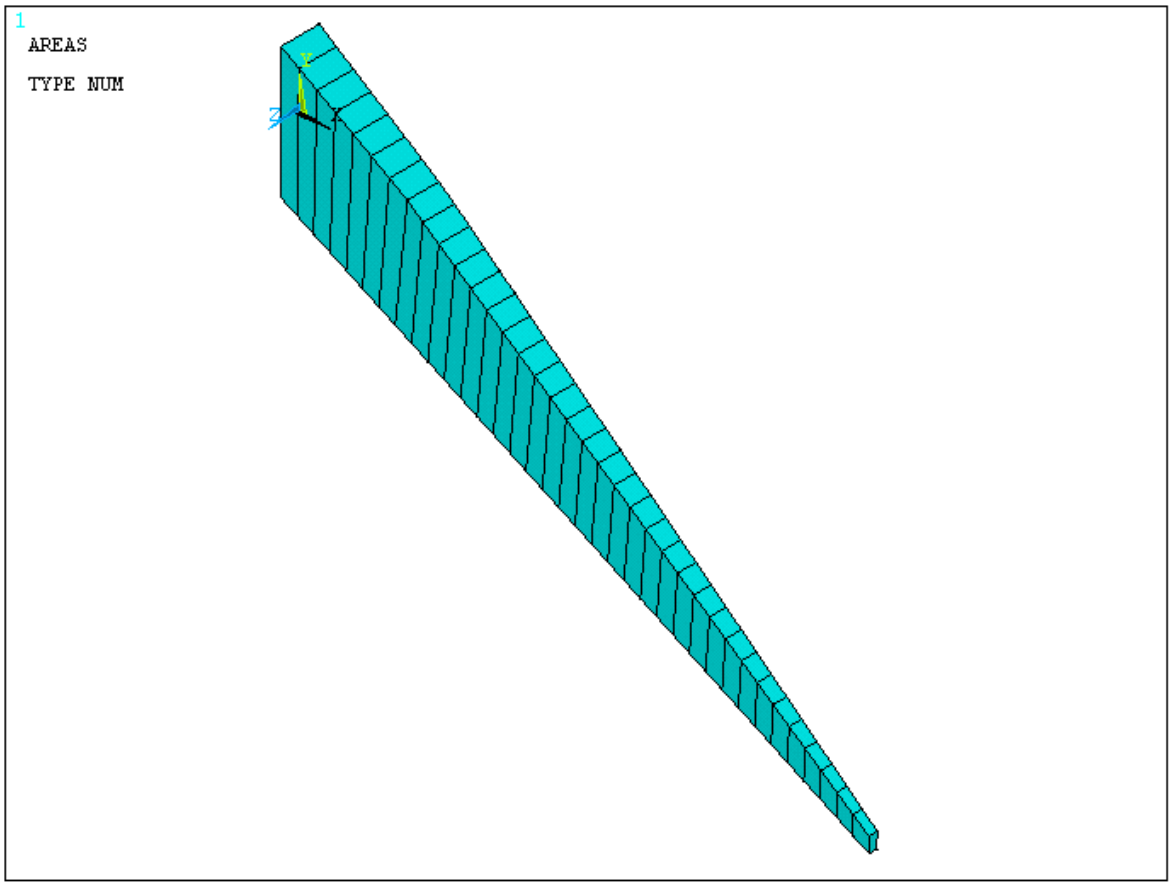

Figure 4-3. ANSYS model of the wingbox

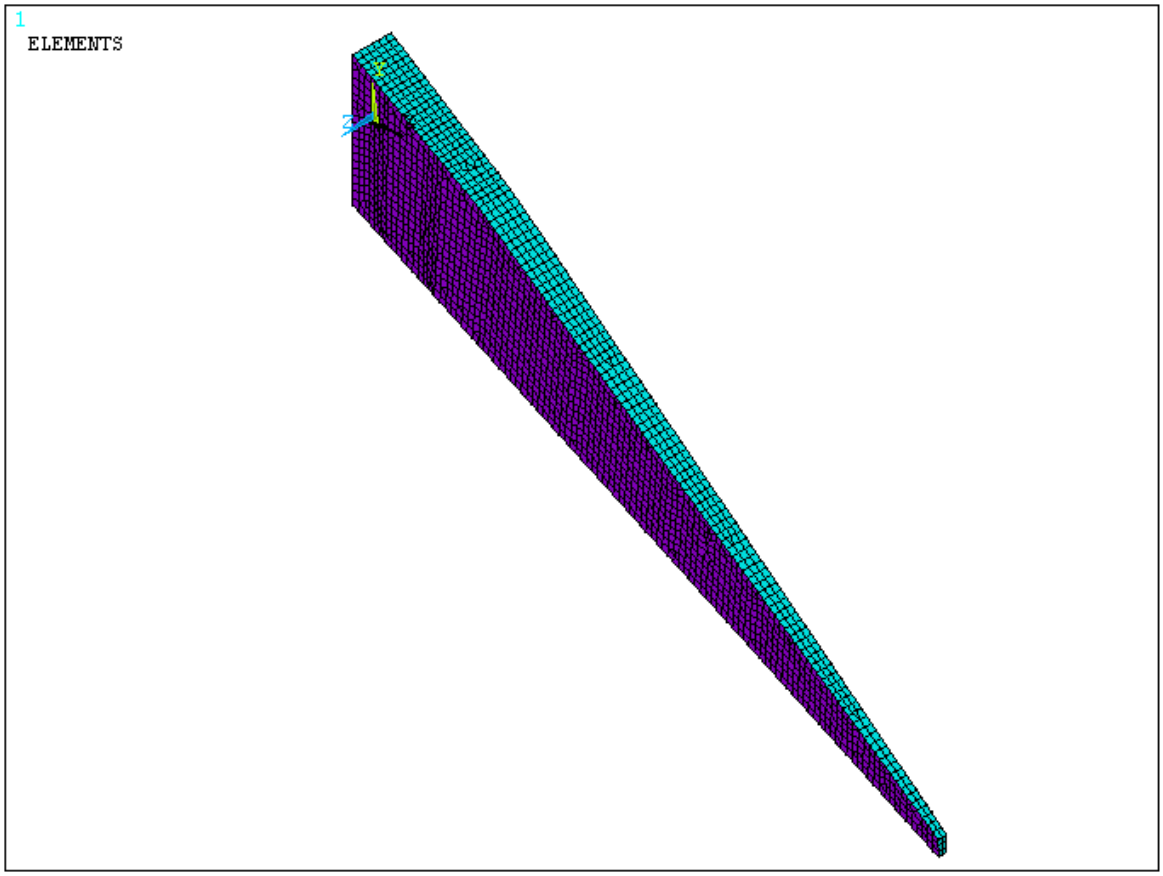

Figure 4-4. Meshed ANSYS model of the wingbox

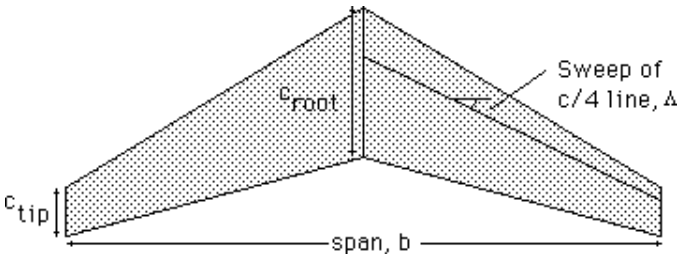

Figure 4-5. Sweep of the quarter-chord

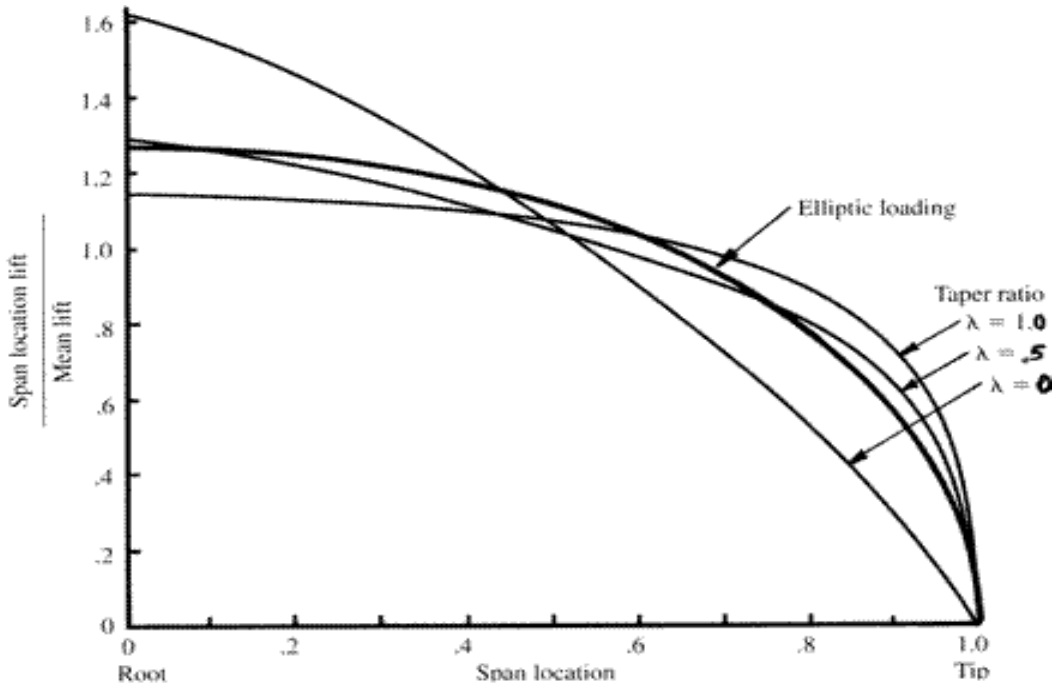

Figure 4-6. Relationship of local lift distribution and taper ratio

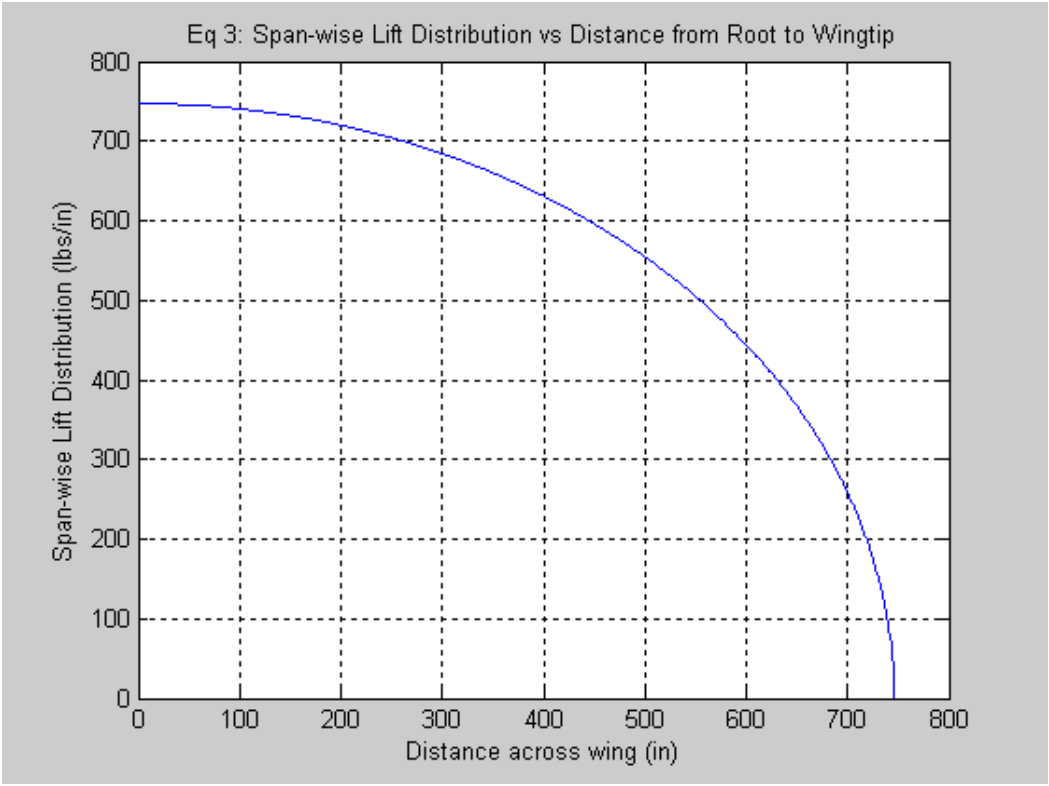

Figure 4-7. Elliptical lift distribution from the root to the tip of the wingbox model

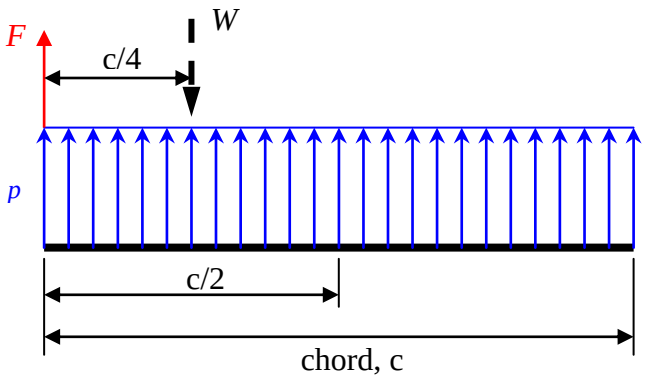

Figure 4-8. Equilibrium of forces on the wingbox model

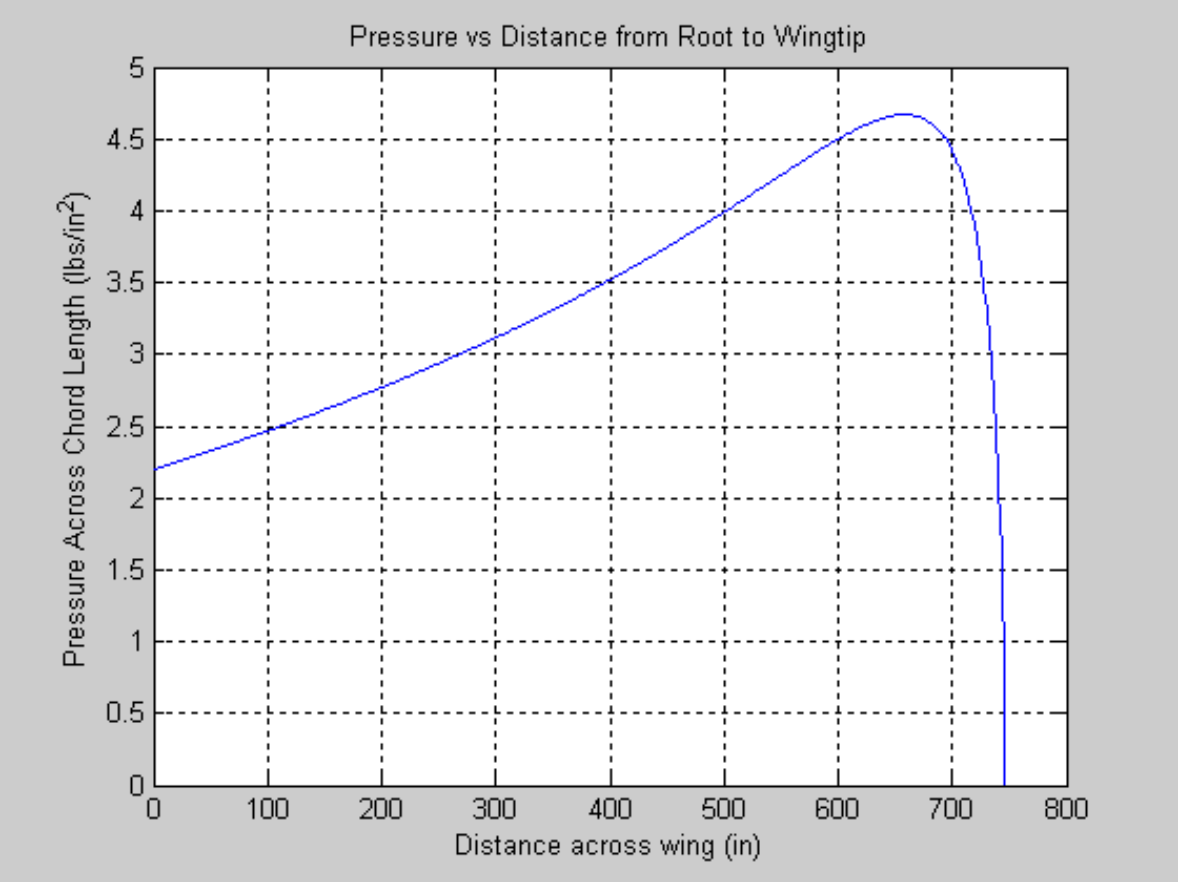

Figure 4-9. Pressure distribution from root to wingtip of the model

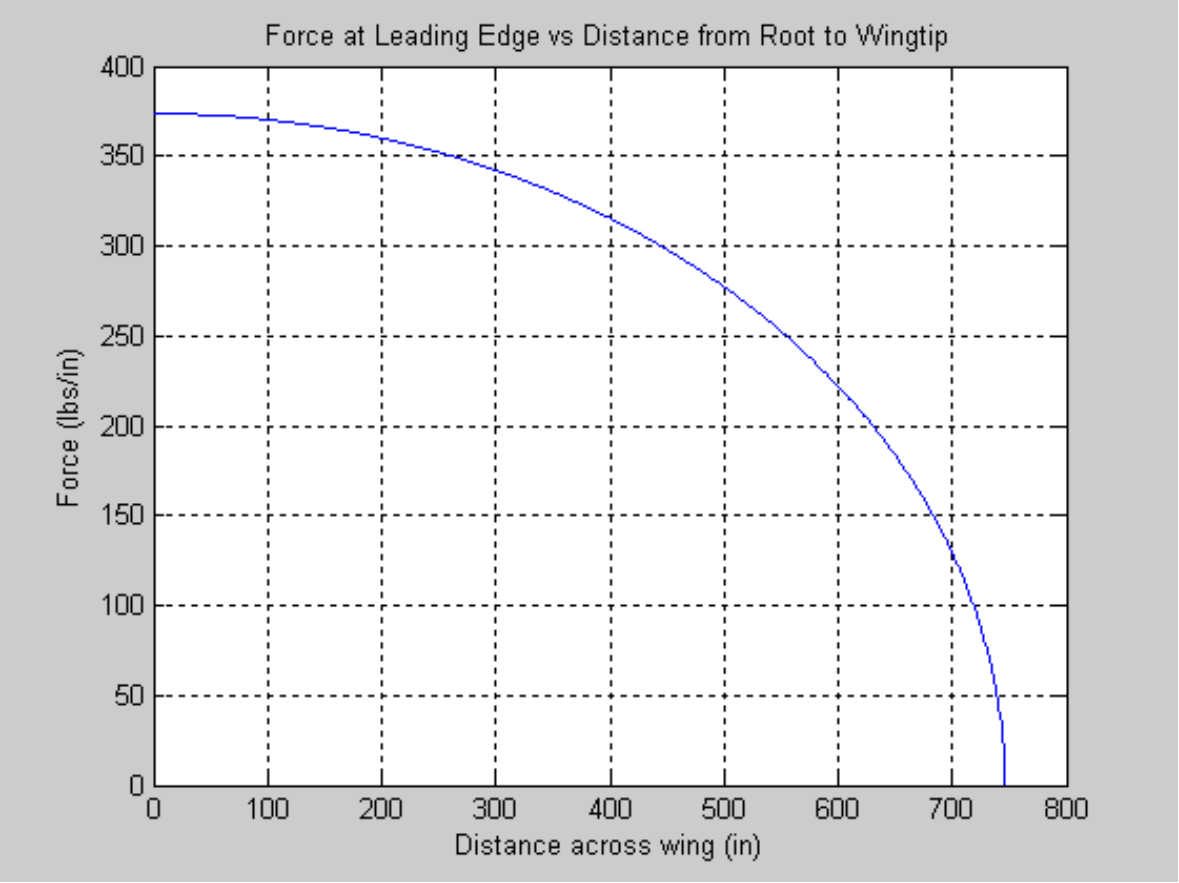

Figure 4-10. Force distribution from root to wingtip of the model

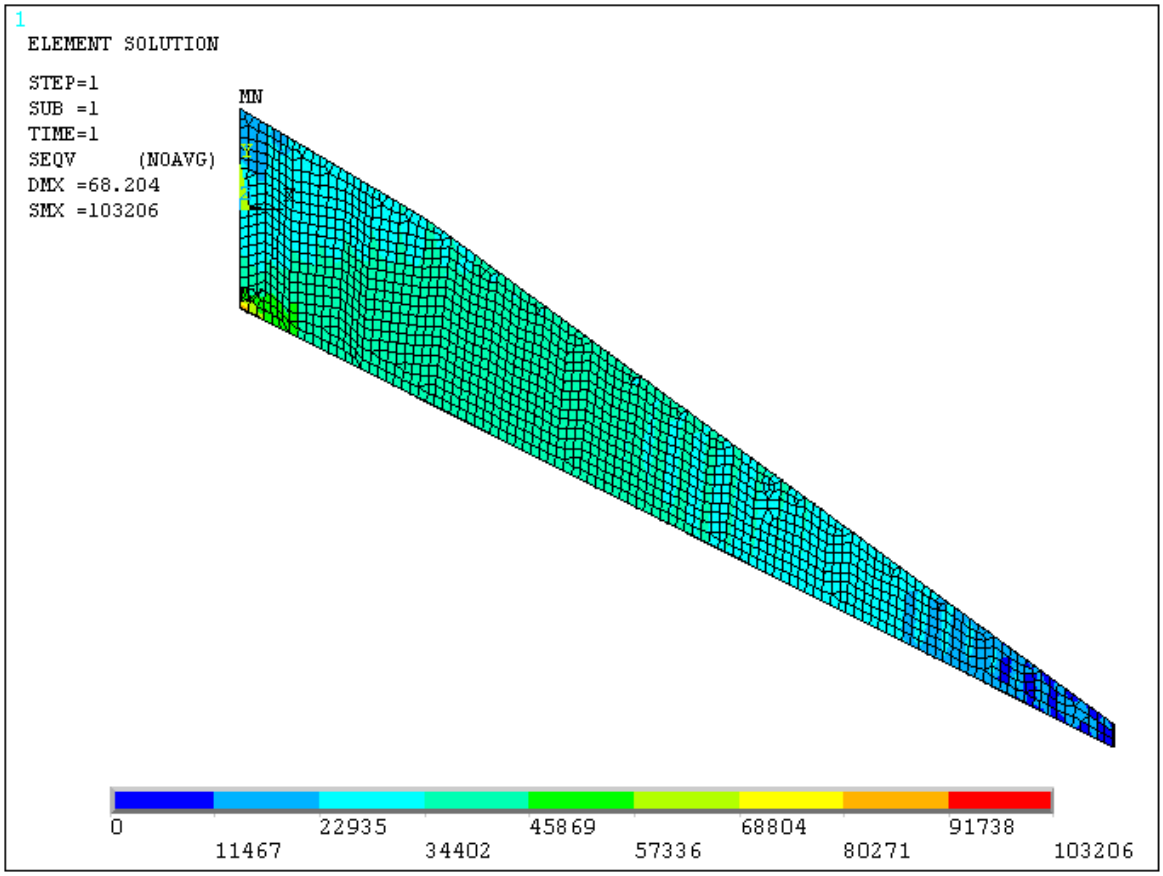

Figure 4-11. Contour plot of maximum stress on the wingbox model

CHAPTER 5
SUMMARY AND CONCLUSIONS

An exact-capacity approximate-response-distribution (ECARD) probabilistic optimization method that dispenses with most of the expensive structural response calculations (typically done via finite element analysis) was proposed in this paper. ECARD was demonstrated with two examples. First, probabilistic optimization of a ten-bar truss problem was performed, where risk was allocated between truss members. Then, probabilistic optimization of a wingbox was performed, where risk was allocated between the different failure modes. From the results obtained in these two demonstration problems, we reached to the following conclusions.

1. In the ten-bar truss problem, ECARD converged to near optima that allocated risk between failure modes much more efficiently than the deterministic optima. The differences between the true and approximate optima were due to the errors involved in probability of failure estimations, which led to errors in the derivatives of probabilities of failure with respect to design variables that is required in risk allocation problems.

2. The approximate optimum required four inexpensive ECARD iterations and five probability of failure calculations for the ten-bar truss example to locate the approximate optimum. In the wingbox example, two ECARD iterations were required and probabilities of failure of the elements are calculated three times to locate the approximate optimum. This represents substantial reduction in the number of probability calculation require for full probabilistic optimization.

APPENDIX
CALCULATION OF MEMBER FORCES OF THE TEN BAR TRUSS

Analytical solution to ten-bar truss problem is given in Elishakoff et al. [16]. The member forces satisfy the following equilibrium and compatibility equations. Note: Values with "*" are incorrect in the reference. The correct expressions are:

$$N_1 = P_2 - \frac{1}{\sqrt{2}} N_8 \tag{A-1}$$

$$N_2 = -\frac{1}{\sqrt{2}} N_{10} \tag{A-2}$$

$$N_3 = -P_1 - 2P_2 - \frac{1}{\sqrt{2}} N_8 \tag{A-3}$$

$$N_4 = -P_2 - \frac{1}{\sqrt{2}} N_{10} \tag{A-4}$$

$$N_5 = -P_2 - \frac{1}{\sqrt{2}} N_8 - \frac{1}{\sqrt{2}} N_{10} \tag{A-5}$$

$$N_6 = -\frac{1}{\sqrt{2}} N_{10} \tag{A-6}$$

$$N_7 = \sqrt{2}\left(P_1 + P_2\right) + N_8 \tag{A-7}$$

$$N_8 * = \frac{b_1 a_{22} - a_{12} b_2}{a_{11} a_{22} - a_{12} a_{21}} \tag{A-8}$$

$$N_9 = \sqrt{2} P_2 + N_{10} \tag{A-9}$$

$$N_{10} * = \frac{a_{11} b_2 - a_{21} b_1}{a_{11} a_{22} - a_{12} a_{21}} \tag{A-10}$$

where

$$a_{11}^{*} = \left(\frac{1}{A_1} + \frac{1}{A_3} + \frac{1}{A_5} + \frac{2\sqrt{2}}{A_7} + \frac{2\sqrt{2}}{A_8} \right) \tag{A-11}$$

$$a_{12}^{*} = a_{21}^{*} = \frac{1}{A_5} \tag{A-12}$$

$$a_{22}^{*} = \left(\frac{1}{A_2} + \frac{1}{A_4} + \frac{1}{A_5} + \frac{1}{A_6} + \frac{2\sqrt{2}}{A_9} + \frac{2\sqrt{2}}{A_{10}} \right) \tag{A-13}$$

$$b_1^{*} = \sqrt{2} \left[\frac{P_2}{A_1} - \frac{P_1 + 2P_2}{A_3} - \frac{P_2}{A_5} - \frac{2\sqrt{2}\left(P_1 + P_2 \right)}{A_7} \right] \tag{A-14}$$

$$b_2^{*} = \left[\frac{-\sqrt{2}P_2}{A_4} - \frac{\sqrt{2}P_2}{A_5} - \frac{4P_2}{A_9} \right] \tag{A-15}$$

LIST OF REFERENCES

[1] Ben Haim, Y., and Elishakoff, I., Convex Models of Uncertainty in Applied Mechanics, Elsevier, Amsterdam, 1990.

[2] Neal, D.M., Matthews, W.T., and Vangel, M.G., "Uncertainties in Obtaining High Reliability from Stress-Strength Models," Proceedings of the 9th DOD/NASA/FAA Conference on Fibrous Composites in Structural Design, Vol. 1, Department of Defense, Lake Tahoe, NV, 1992, pp. 503-521.

[3] Lee, T.W and Kwak, B.M., "A Reliability-based Optimal Design Using Advanced First Order Second Moment Method," Mechanics of Structures and Machines, Vol. 15, No. 4, 1987, pp. 523-542.

[4] Kiureghian, A.D., Zhang, Y., and Li, C.C., "Inverse Reliability Problem," Journal of Engineering Mechanics, Vol. 120, No. 5, 1994, pp. 1154-1159.

[5] Tu, J., Choi, K.K., and Park, Y.H., "A New Study on Reliability Based Design Optimization," ASME Journal of Mechanical Design, Vol. 121, No. 4, 1999, pp. 557-564.

[6] Lee, J.O., Yang, Y.S., Ruy, W.S., "A Comparative Study on Reliability-index and Target-performance-based Probabilistic Structural Design Optimization," Computers and Structures, Vol. 80, No. 3-4, 2002, pp. 257-269.

[7] Qu, X., and Haftka, R.T., "Reliability-based Design Optimization Using Probabilistic Sufficiency Factor," Journal of Structural and Multidisciplinary Optimization, Vol. 27, No.5, 2004, pp. 314-325.

[8] Du, X., and Chen, W., "Sequential Optimization and Reliability Assessment Method for Efficient Probabilistic Design," ASME Journal of Mechanical Design, Vol. 126, No. 2, 2004, pp. 225-233.

[9] Ba-abbad, M.A., Nikolaidis, E., and Kapania, R.K., "New Approach for System Reliability-Based Design Optimization," AIAA Journal, Vol. 44, No. 5, May 2006, pp. 1087-1096.

[10] Mogami, K., Nishiwaki, S., Izui, K, Yoshimura, M., and Kogiso, N., "Reliability-based Structural Optimization of Frame Structures for Multiple Failure Criteria Using Topology Optimization Techniques," in press, Structural and Multidisciplinary Optimization, 2006.

[11] Acar, E., Kumar S., Pippy R.J., Kim N.H., Haftka R. T., "Approximate Probabilistic Optimization Using Exact-Capacity-Approximate-Response-Distribution (ECARD)", submitted, 48th AIAA/ASME/ASCE/AHS/ASC Structures, Structural Dynamics, and Materials Conference, 2006.

[12] Oberkampf, W.L., DeLand, S.M., Rutherford, B.M., Diegert, K.V. and Alvin, K.F., "Estimation of Total Uncertainty in Modeling and Simulation", Sandia National Laboratory Report, SAND2000-0824, Albuquerque, NM, April 2000.

[13] Oberkampf, W.L., Deland, S.M., Rutherford, B.M., Diegert, K.V., and Alvin, K.F., "Error and Uncertainty in Modeling and Simulation," Reliability Engineering and System Safety, Vol. 75, 2002, pp. 333-357.

[14] Acar, E., Kale, A. and Haftka, R.T., "Effects of Error, Variability, Testing and Safety Factors on Aircraft Safety," Proceedings of the NSF Workshop on Reliable Engineering Computing, 2004, pp. 103-118.

[15] Acar, E., Kale, A., and Haftka, R.T., "Comparing Effectiveness of Measures that Improve Aircraft Structural Safety," submitted, ASCE Journal of Aerospace Engineering, 2006.

[16] Haftka, R.T., and Gurdal, Z., "Elements of Structural Optimization," Kluwer Academic Publishers, 3rd edition, 1992.

[17] Elishakoff, I., Haftka, R.T., and Fang, J., "Structural Design Under Bounded Uncertainty—Optimization with Anti-optimization," Computers and Structures, Vol. 53, No. 6, 1994, pp. 1401-1405.

[18] Smarslok, B.P., Haftka, R.T., and Kim, N.H., "Taking Advantage of Separable Limit States in Sampling Procedures," AIAA Paper 2006-1632, 47th AIAA/ASME/ASCE/AHS/ASC Structures, Structural Dynamics, and Materials Conference, Newport, RI, May 2006.

[19] Kreyzig E., Advanced Engineering Mathematics, Wiley, New York, pp. 848.

[20] Haftka, R.T., and Gurdal, Z., "Elements of Structural Optimization," Kluwer Academic Publishers, 3rd edition, 1992.

[21] Richard C. Rice, Jana L. Jackson, John Bakuckas, and Steven Thompson, "Metallic Material Properties Development and Standardization (MMPDS)," Federal Aviation Administration, January 2003.

BIOGRAPHICAL SKETCH

Richard Pippy was born in Bronxville, New York, in 1972. Upon graduation from high school, he joined the United States Marine Corps, where he served for six years. After his honorable discharge, he then attended St. Petersburg College where he received an Associate of Arts degree in 2001. He then joined the University of Florida, where he earned a Bachelor of Science degree in mechanical engineering in 2005. In 2006, he returned to the University of Florida to pursue a master's degree in mechanical engineering. Under the supervision of Dr. Nam-Ho Kim, he earned his master's degree in 2008.